

Research Article

UPFC Location and Performance Analysis in Deregulated Power Systems

Seyed Abbas Taher and Ali Akbar Abrishami

Department of Electrical Engineering, University of Kashan, Kashan, Iran

Correspondence should be addressed to Seyed Abbas Taher, sataher@kashanu.ac.ir

Received 13 May 2009; Revised 17 October 2009; Accepted 21 November 2009

Recommended by Wei-Chiang Hong

We deal with the effect of Unified Power Flow Controller (UPFC) installation on the objective function of an electricity market. Also this paper proposes a Novel UPFC modelling in OPF which facilitates the consideration of the impact of four factors on power market. These include the series transformer impedance addition, the shunt reactive power injection, the in-phase component of the series voltage and the quadrature component of the series voltage. The impact of each factor on the electricity market objective function is measured and then compared with the results from a sensitivity approach. The proposed sensitivity approach is fast so it does not need to repeat OPF solutions. The total impacts of the factors are used to offer UPFC insertion candidate points. It is shown that there is a clear match between the candidate points of the sensitivity method and those proposed by the introduced UPFC modelling in our test case. Furthermore, based on the proposed method, the relation between settings of UPFC series part and active and reactive power spot prices is presented.

Copyright © 2009 S. A. Taher and A. A. Abrishami. This is an open access article distributed under the Creative Commons Attribution License, which permits unrestricted use, distribution, and reproduction in any medium, provided the original work is properly cited.

1. Introduction

Limitations in transmission and generation system expansion, such as right-of-way and environmental problems, have made it inevitable to use the current network capacity as much as possible [1]. The competition in a restructured power system leads to its optimization and new ways for cost reduction. Flexible AC Transmission Systems (FACTS), which are developed as a result of recent progress in power electronic technology and communication systems, have opened alternative ways of increasing loadability, better network control and cost reduction. FACTS devices can be used for congestion management [2], energy loss minimization [3], power flow control [4], security enhancement [1], social welfare maximization [5] and network stability improvement [6].

To manage power pricing in a PoolCo power market, an ISO implements Optimal Power Flow (OPF) in which the main objective is to maximize social welfare subject to

some network constraints [7, 8]. FACTS settings in steady state applications are determined together with optimal power flow variables in a single unified framework. In some electricity markets, ISO may own all FACTS devices. In this case, it is responsible for both their operation and planning. On the other hand, in some electricity markets, FACTS devices may be owned by different entities that are paid by ISO based on "Ancillary Services" they provide for ISO. In this case, also, ISO controls FACTS devices; but studies related to FACTS planning, which we deal with in this paper, is a subject of interest for FACTS investors.

Among FACTS devices, the Unified Power Flow Controller (UPFC) is able to simultaneously compensate reactive power and control active and reactive power flows of a transmission line [9]. By employing UPFCs, electricity generation cost and active power losses can be reduced [1, 10]. Using a UPFC in a power market in order to minimize the market cost may lead to the reduction in spot prices of load buses [5]. Both real and reactive power spot prices may subsequently change drastically. An impact on transmission cost allocation in a power market, as a result of UPFC operation, has been reported in [11]. In spite of the above mentioned steady state effects of UPFCs, to the best of our knowledge, no discussion has so far been presented about the desired UPFC settings from an OPF solution and the effect of each of the UPFC functions, including shunt reactive power compensation and active and reactive power flow control.

In this paper, a proposed detailed UPFC modeling, including internal UPFC state and control variables and serial and shunt impedances, is incorporated in the OPF formulation. Through that, the factors influencing the objective function of an electricity market resulting from UPFC installation, namely, the series transformer impedance insertion, the shunt reactive injection, the in-phase component of the series voltage and the quadrature component of the series voltage have taken into account. Also, to measure the impact of these components on improving the objective function of an electricity market, two approaches, namely a differencing method and a sensitivity analysis, are presented. The above four impacts are added in each case to identify the potential points for UPFC installation. The sensitivity approach is fast as it needs to run OPF only once in the base case system without UPFC, to derive the sensitivity coefficients. Therefore, the computational burden in more accurate UPFC allocation techniques such as [12–14] could be significantly decreased if this approach is used to limit the search space. The relation between UPFC series part settings and Locational Marginal Prices (LMP) is another subject presented in this paper.

This paper is organized as follows: In Section 2, optimal power flow and its implementation are presented. Incorporation of the UPFC modelling in OPF is described in Section 3. Then in Section 4, to validate the proposed approaches, a UPFC is placed on all possible points of a test system and the impacts of all pre-mentioned components on improving the objective function of an electricity market are computed by the two approaches. UPFC allocation is also discussed in this section. Finally, concluding remarks are presented in Section 5.

2. Optimal Power Flow Implementation

The main objective of an electricity market is to maximize the social welfare which consists of bid prices of generation units and loads [8]. For the sake of simplicity, customers' loads are assumed to be constant. However, consideration of more accurate load models and bid prices of customers are also possible. The mathematical formulation of an optimal power

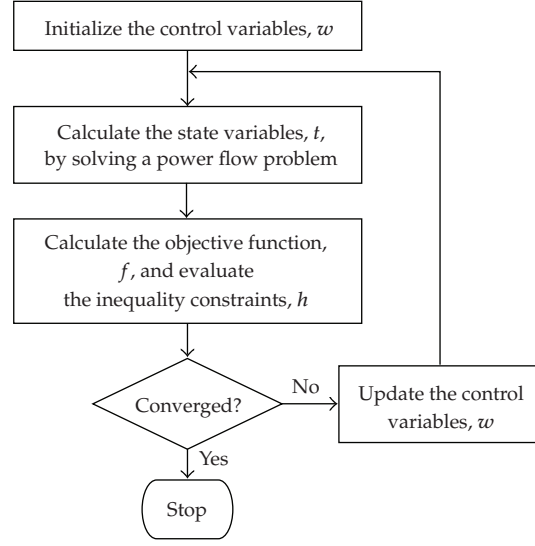


Figure 1: Optimal power flow implementation outline.

flow problem can be expressed as

$$\begin{aligned}
 & \text{Min } f(t, w), \\
 & \text{subject to } g(t, w) = 0, \\
 & \quad \quad \quad h(t, w) \leq 0,
 \end{aligned} \tag{2.1}$$

where the cost function, f , is the total bid offers of the generators. Note that since we have assumed that the price elasticity of demand is zero, minimizing f is equivalent to maximizing the welfare [8]; when no UPFC is installed the control variables, w , are active power generations, P_G , and reactive power generations, Q_G . The state variables, t , include load bus voltages, V_L , and load bus angles, θ_L . The equality constraints, g , in the optimization are nonlinear AC load flow equations. The inequality constraints, h , are as following.

$$P_{Gi}^{\min} \leq P_{Gi} \leq P_{Gi}^{\max} \quad \text{Upper and lower active powers of generator-}i,$$

$$Q_{Gi}^{\min} \leq Q_{Gi} \leq Q_{Gi}^{\max} \quad \text{Upper and lower reactive powers of generator-}i,$$

$$V_G^{\min} \leq V_{Gi} \leq V_G^{\max} \quad \text{Upper and lower voltage magnitudes of generator-}i,$$

$$I_{i-j} \leq I_{i-j}^{\max} \quad \text{Maximum allowable current of line } i-j,$$

$$V_L^{\min} \leq V_{Li} \leq V_L^{\max} \quad \text{Upper and lower voltage magnitudes of load bus-}i.$$

In this paper the optimal power flow solution is based on separating the control variables, w , from the state variables, t [15]. The algorithm of optimal power flow is shown in Figure 1.

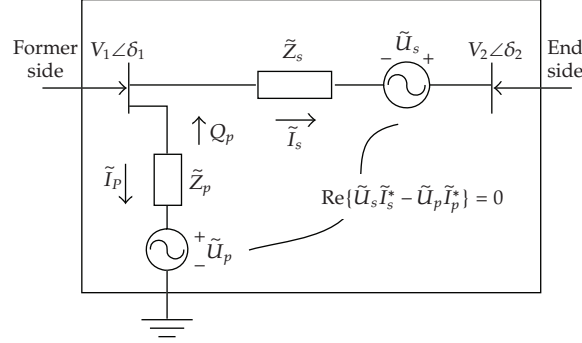


Figure 2: UPFC equivalent circuit.

3. UPFC Modelling and Performance Analysis in a Power Market

3.1. Novel UPFC Modelling in OPF

The Acha's UPFC modelling [10, 16] consists of two voltage sources and two impedances representing the series and the shunt converters and transformers in a UPFC, as shown in Figure 2 where

- (i) \tilde{Z}_s and \tilde{Z}_p represent series and shunt transformers leakage impedances, respectively
- (ii) \tilde{I}_s and \tilde{I}_p denote series and shunt converter currents, respectively
- (iii) Q_p is the net shunt reactive power injected to the former side bus

The UPFC control parameters in [10, 16] modelling are the amplitude and the angle of the series converter voltage phasor (U_s, φ_s) and the amplitude and the angle of the shunt converter voltage phasor (U_p, φ_p). However, none of these control parameters are directly effective in active or reactive power flow from UPFC converters. Thus, it makes this model inappropriate to use for a performance analysis. In this paper, that modelling is enhanced to resolve this issue. The UPFC control parameters of proposed model include the in-phase and quadrature components of the series converter voltage (U_{sx}, U_{sy}) as shown in Figure 3(a), and the in-phase and quadrature components of the shunt converter voltage (U_{px}, U_{py}) as shown in Figure 3(b). U_{sx} and U_{px} are at the same angle as \tilde{V}_1 while U_{sy} and U_{py} are perpendicular to \tilde{V}_1 . These parameters can mathematically be expressed as

$$\begin{aligned}\tilde{U}_s &= (U_{sx} + jU_{sy}) \times e^{j\delta_1}, \\ \tilde{U}_p &= (U_{px} + jU_{py}) \times e^{j\delta_1}.\end{aligned}\tag{3.1}$$

Under normal operating conditions of a power system, $\delta_1 - \delta_2$ and $V_1 - V_2$ are small and the resistances of \tilde{Z}_s and \tilde{Z}_p are small, as well. Thus it can be supposed that, U_{sx} and U_{sy} influence only reactive power flow and active power flow from bus 1 to bus 2, respectively. In other words, the in-phase and the quadrature components of the UPFC series voltage are comparable in operation to a tap changer and a phase-shifter, respectively (Figure 3(a)).

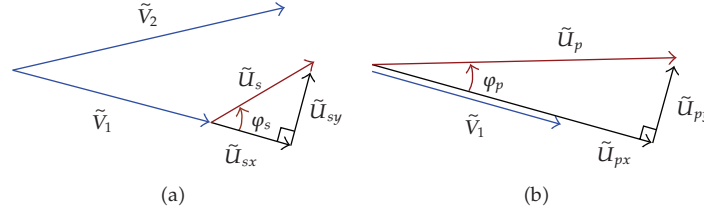


Figure 3: Phasor diagrams of (a) series converter and (b) shunt converter voltages.

On the other hands U_{px} and U_{py} are responsible for flowing the reactive and active powers, respectively, in the shunt part of the UPFC equivalent circuit in Figure 2.

In order to incorporate the proposed UPFC model into the OPF algorithm, three UPFC parameters, namely, U_{sx} , U_{sy} and U_{px} , should be added to the set of the optimization control variables, w , and at the same time, the only remaining parameter, U_{py} , should be added to the set of the state variables, t . According to U_{py} function, this parameter is incorporated into the Jacobian matrix and mismatch equations of the load flow to satisfy the active power balance equation in the UPFC. Also, the UPFC operational limits given below should be added to the optimization inequalities, h .

$$I_s \leq I_s^{\max} \quad \text{Maximum current of the series part}$$

$$I_p \leq I_p^{\max} \quad \text{Maximum current of the shunt part}$$

$$U_s \leq U_s^{\max} \quad \text{Maximum series voltage magnitude}$$

$$U_p \leq U_p^{\max} \quad \text{Maximum shunt voltage magnitude.}$$

3.2. UPFC Performance Analysis in a Power Market

The UPFC model is composed of two voltage sources and two impedances, representing physical converters and transformers. To determine how much the installation of a UPFC may affect a power system, we can include the components of the UPFC model, one by one, and accordingly, study the effect of each. First, we import the series and shunt impedances. Note that the resistances of the transformers can be neglected as they are much smaller than their reactances. Then, the series voltage components are enabled. U_{sx} and U_{sy} are independent variables and enabling them has an impact on the system. On the other hand, among the shunt voltage components, U_{px} has a similar behaviour and could be treated similarly. However, U_{py} is a dependent variable and is modified according to the other three control variables, to keep the active power balance in the UPFC. So, once for instance, U_{sx} is enabled, U_{py} would change accordingly and therefore, its effect would be taken into account and as such needs not to be calculated separately. Besides, some part of the shunt reactive power produced due to enabling U_{px} is lost in the shunt impedance, \tilde{Z}_p , which can be considered as the main influence of \tilde{Z}_p . Therefore, the effects of U_{px} and the shunt impedance can be combined if, instead, we consider the net reactive power injected to the former side bus, Q_p .

In brief, the influence of UPFC installation on a power market can be considered as the total impacts of four functions.

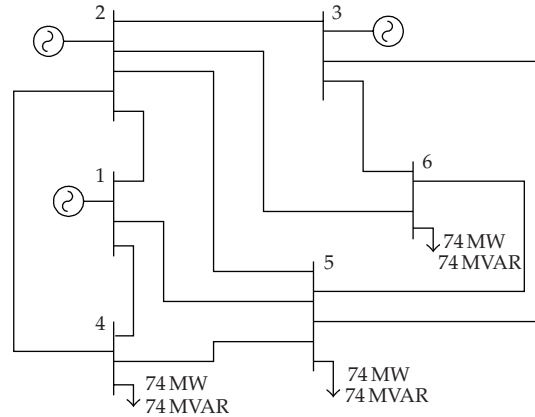


Figure 4: Six bus test system diagram.

- (i) The insertion of the UPFC series transformer impedance on the line
- (ii) Reactive power injection, Q_p , at the former side bus due to U_{px}
- (iii) Reactive power flow in the series part due to U_{sx}
- (iv) Active power flow in the series part due to U_{sy}

The series transformer impedance addition regularly increases the OPF objective function since it increases the line impedance. The next three components are the variables of the optimization and should decrease the objective function.

3.3. The Relation between UPFC Series Voltage Components and LMPs

In an electricity power market, when the power price (active LMP) at the sending end of a transmission line is cheaper than the one at the receiving end, flowing the active power from the sending end to the receiving end is desirable. In this case, given a UPFC installed at the sending end of the line, U_{sy} should be set at a positive value to produce this flow and vice versa. Likewise, this rule is also true about the reactive power. That is to say, if the reactive LMP at the sending end of the transmission line is less than the one at the receiving end, U_{sx} ought to be set at a positive value to cause this flow and vice versa. If the maximum thermal current of the line is reached in the base case, UPFC series parameters are, however, set in a different manner. U_{sx} and U_{sy} settings should be so selected in this case to decrease the line current.

4. Case Studies and Results Analysis

Validation tests are performed on the six bus 11 lines test system shown in Figure 4 [7]. The system consists of three generating units at buses 1 through 3 and three loads at buses 4 through 6. The bid prices of generating units are selected based on typical values in 2004. The OPF results of the test system are summarized in Table 1. The OPF cost in this electricity market, f , is 8815.09 \$/hr. The reactive power generation of G3, Q_{G3} , and the current at the receiving ends of line 2-4 and line 1-5, I_{4-2} and I_{5-1} , are set to their maximum values.

Table 1: Electricity market generation schedule in the six bus system without UPFC.

Gen bus	P (MW)	Q (MVAR)	V (pu)	Binding Constraints
1	73.88	69.41	1.05	Q_{G3}^{\max} I_{l4-2}^{\max} I_{l5-1}^{\max}
2	69.13	67.56	1.021	cost function
3	87.15	60.00	1.018	$f = 8815.09 \text{ \$/hr}$

In order to allocate UPFCs in a system, all possible locations should be evaluated and the number, location and size of the UPFCs should be determined. The possibility of installing the UPFCs at both ends of all lines in the six bus system is considered which constitutes 22 cases. Then, the optimal power flow problem is solved for these installation cases and finally, the OPF costs are compared.

With reference to the size, the maximum UPFC series voltage can be up to 0.5 pu of the line voltage [17] or even more. This determines the series converter MVA. Also, the series and shunt converters may [17] or may not [12] have the same size. Determination of converter MVAs is a matter of UPFC allocation. In this paper, however, we would like to find some areas as candidate points for UPFC installation by performing a sensitivity analysis. Once the promising candidate points are determined by this approach, more precise UPFC allocation algorithms such as [12, 13] would be necessary to select the final points. So, with regard to the purpose of this paper, the UPFC series and shunt converters are sized into the relatively small fixed value of 4 MVA, equal to 0.04 pu with $S_{\text{base}} = 100$ MVA. Since the current ratings of the test system lines are 0.4 pu on average, the UPFC maximum series voltage would be typically 0.1 pu. Also, the assumption of constant sized converters removes the need to calculate the UPFC investment cost.

Apart from the size of converters, other UPFC ratings may vary at different points. The maximum voltage magnitude of the shunt converter, U_p^{\max} , is always a bit more than the line nominal voltage. Here, it is chosen 1.2 pu in all cases. Since U_p is normally about 1.0 pu, the maximum current of the shunt converter, I_p^{\max} , will be the same as the converter apparent power rating, 0.04 pu, in all cases. The maximum current of the series part, I_s^{\max} , is practically selected to be equal to the line current thermal limit [17]. Given the nominal power and the maximum current of the series converter, the maximum voltage magnitude of the series converter, U_s^{\max} , is

$$U_s^{\max} = \frac{\text{MVA}_{\text{series}}}{I_s^{\max}}. \quad (4.1)$$

The resistances and the reactances of the coupling transformers are chosen from typical figures based on their voltage level and nominal power.

A differencing method which includes the following steps, applied to all 22 UPFC placement cases.

- (i) By letting three UPFC control parameters free, run optimal power flow and obtain UPFC settings (U_{px}^* , U_{sx}^* and U_{sy}^*) and OPF cost function, f_{opf}^4 .
- (ii) Use UPFC in zero compensation mode ($Q_p = 0$, $U_{sx} = 0$ and $U_{sy} = 0$) and obtain OPF cost function, f_{opf}^1 .

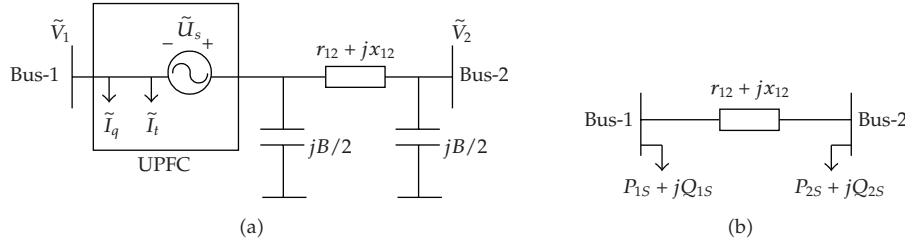


Figure 5: UPFC equivalent circuit and power injection model [5].

- (iii) Use UPFC in the operating mode (Q_p free, $U_{sx} = 0$ and $U_{sy} = 0$) and obtain OPF cost function, f_{opf}^2 .
- (iv) Use UPFC in the operating mode (Q_p free, $U_{sx} = U_{sx}^*$ and $U_{sy} = 0$) and obtain OPF cost function, f_{opf}^3 .

In each step, one of the four UPFC elements effective in changing the OPF cost function is added. Then, the objective function of the step, f_{opf}^k , is obtained by the OPF solution. So the OPF cost function alteration caused by adding an element y_k , Δf_{difr}^k , can be computed as

$$\Delta f_{\text{difr}}^k = f_{\text{opf}}^k - f_{\text{opf}}^{k-1}, \quad k = 1, \dots, 4, \quad (4.2)$$

where the OPF cost for the base case system with no UPFC, f_{opf}^0 , is 8815.09\$/hr as given in Table 1. The change in the OPF cost function due to enabling an element y_k can also be calculated by a sensitivity analysis, Δf_{sens}^k , as shown in (4.3).

$$\Delta f_{\text{sens}}^k = \frac{\partial f}{\partial y_k} \times y_k^*, \quad k = 1, \dots, 4, \quad (4.3)$$

where y_1^* is the series transformer leakage impedance; y_2^* denotes the net reactive power injected by the shunt converter, Q_p ; y_3^* and y_4^* are the in-phase and the quadrature components of the series voltage, respectively, obtained in step I; $\partial f / \partial y_k$ is the OPF cost function sensitivity with respect to the element y_k . The sensitivity factors are calculated using the OPF results of the main system with no UPFC.

The sensitivity of OPF objective function with respect to shunt converter reactive power injection, $\partial f / \partial Q_p$, is equal to the reactive LMP at the bus to which the UPFC is connected. Active and reactive LMPs are the Lagrangian multipliers of power flow equations in optimal power flow, which are obtained after solving OPF. $\partial f / \partial U_{sx}$ and $\partial f / \partial U_{sy}$ coefficients can be calculated using Figure 5. Suppose that a UPFC is installed at the sending end of line 1-2. Figure 5(a) shows the equivalent circuit of the UPFC [5] in which I_t and I_q are the in-phase and the quadrature components of the shunt converter current with respect to \tilde{V}_1 .

Injecting powers P_{1S} , Q_{1S} , P_{2S} and Q_{2S} in Figure 5(b) is equal to UPFC insertion on the sending end of line 1-2 in Figure 5(a). These powers can be represented in terms of U_{sx} , U_{sy} and I_q as

$$P_{1S} = -g_{12}(U_{sx}^2 + U_{sy}^2) - 2g_{12}V_1U_{sx} + g_{12}V_2(U_{sx} \cos \Delta\delta - U_{sy} \sin \Delta\delta) + b_{12}V_2(U_{sx} \sin \Delta\delta + U_{sy} \cos \Delta\delta), \quad (4.4)$$

$$Q_{1S} = g_{12}V_1U_{sy} + \left(b_{12} + \frac{B}{2}\right)V_1U_{sx} + V_1I_q, \quad (4.5)$$

$$P_{2S} = g_{12}V_2(U_{sx} \cos \Delta\delta - U_{sy} \sin \Delta\delta) - b_{12}V_2(U_{sx} \sin \Delta\delta + U_{sy} \cos \Delta\delta), \quad (4.6)$$

$$Q_{2S} = -g_{12}V_2(U_{sx} \sin \Delta\delta + U_{sy} \cos \Delta\delta) - b_{12}V_2(U_{sx} \cos \Delta\delta - U_{sy} \sin \Delta\delta). \quad (4.7)$$

The consequence of these power injections in changing OPF cost function can be estimated by LMPs. In order to compute $\partial f / \partial U_{sx}$, the variables U_{sy} and I_q in (4.4)–(4.7) are set to zero and the chain rule is used as

$$\begin{aligned} \frac{\partial f}{\partial U_{sx}} &= \frac{\partial P_{1S}}{\partial U_{sx}} \cdot \text{ALMP}_1 + \frac{\partial Q_{1S}}{\partial U_{sx}} \cdot \text{RLMP}_1 + \frac{\partial P_{2S}}{\partial U_{sx}} \cdot \text{ALMP}_2 \\ &+ \frac{\partial Q_{2S}}{\partial U_{sx}} \cdot \text{RLMP}_2 + \frac{\partial I_{1-2}}{\partial U_{sx}} \cdot \lambda_{I_{1-2}} + \frac{\partial I_{2-1}}{\partial U_{sx}} \cdot \lambda_{I_{2-1}}, \end{aligned} \quad (4.8)$$

where ALMP_1 , RLMP_1 , ALMP_2 and RLMP_2 are the active and the reactive LMPs at line 1-2 both ends. Also, $\partial I_{1-2} / \partial U_{sx}$ and $\partial I_{2-1} / \partial U_{sx}$ are the derivatives of the current through line 1-2 with respect to U_{sx} ; likewise, $\lambda_{I_{1-2}}$ and $\lambda_{I_{2-1}}$ are the Lagrangian multipliers of the maximum current constraints at the sending and the receiving ends of line 1-2. However, the last two terms in (4.8) may seem to be irrelevant. The reason these terms are added can be explained as follows: UPFC series voltage causes the line current to change. This change, when the maximum line current is binding, produces a second change in OPF cost which can be estimated using the maximum current Lagrangian multiplier. In our test case, nonetheless, the maximum current multiplier only at the receiving end of line 2-4 and at the receiving end of line 1-5 is nonzero. $\partial I_{1-2} / \partial U_{sx}$ in (4.8) can be simply derived based on the definition of I_{1-2} .

$$\frac{\partial I_{1-2}}{\partial U_{sx}} = \frac{1}{S_{11-2} \cdot V_1} \left(P_{12\text{old}} \cdot \frac{\partial P_{1S}}{\partial U_{sx}} + Q_{12\text{old}} \cdot \frac{\partial Q_{1S}}{\partial U_{sx}} \right), \quad (4.9)$$

where S_{11-2} , $P_{12\text{old}}$ and $Q_{12\text{old}}$ are the apparent, active and reactive powers of line 1-2 while U_{sx} , U_{sy} and I_q are set to zero. A similar procedure can be employed to calculate $\partial f / \partial U_{sy}$ (i.e., let U_{sx} and I_q be zero and use an equation similar to (4.8)).

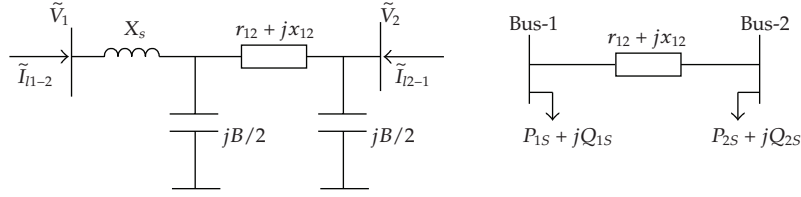


Figure 6: Equivalent circuit of UPFC series transformer impedance and power injection model.

$\partial f / \partial X_s$ can be calculated by substituting power injections P_{1S} , Q_{1S} , P_{2S} and Q_{2S} for the series transformer impedance, X_s , as shown in Figure 6. In a similar way to (4.8), we obtain for X_s

$$\begin{aligned} \frac{\partial f}{\partial X_s} &= \frac{\partial P_{1S}}{\partial X_s} \cdot \text{ALMP}_1 + \frac{\partial Q_{1S}}{\partial X_s} \cdot \text{RLMP}_1 + \frac{\partial P_{2S}}{\partial X_s} \cdot \text{ALMP}_2 \\ &+ \frac{\partial Q_{2S}}{\partial X_s} \cdot \text{RLMP}_2 + \frac{\partial I_{1-2}}{\partial X_s} \cdot \lambda_{I_{1-2}} + \frac{\partial I_{2-1}}{\partial X_s} \cdot \lambda_{I_{2-1}}, \end{aligned} \quad (4.10)$$

where $\partial I_{1-2} / \partial X_s$ is calculated by an equation similar to (4.9). After calculating the injection powers in Figure 6, the derivatives in (4.10) are obtained as:

$$\begin{aligned} \frac{\partial P_{1S}}{\partial X_s} &= \left(\frac{B}{2} + b_{12} \right) \cdot P_{12\text{old}} - g_{12} \cdot Q_{12\text{old}} \\ \frac{\partial Q_{1S}}{\partial X_s} &= \left(\frac{B}{2} + b_{12} \right) \cdot Q_{12\text{old}} + g_{12} \cdot P_{12\text{old}} \\ \frac{\partial P_{2S}}{\partial X_s} &= \left(\frac{B}{2} + b_{12} \right) \cdot P_{21\text{old}} - g_{12} \cdot Q_{21\text{old}} - B \cdot g_{12} V_2^2 \\ \frac{\partial Q_{2S}}{\partial X_s} &= \left(\frac{B}{2} + b_{12} \right) \cdot Q_{21\text{old}} + g_{12} \cdot P_{21\text{old}} + \left(\frac{B}{2} + 2b_{12} \right) \cdot \frac{B}{2} \cdot V_2^2. \end{aligned} \quad (4.11)$$

The values of $\partial f / \partial y_k$, y_k^* and Δf_{sens}^k for $k = 1, \dots, 4$ are shown in Tables 2 through 5 and compared with the differencing results, $\Delta f_{\text{diffr}}^k$. It can be seen that Δf_{sens}^k provides a reasonable estimation of $\Delta f_{\text{diffr}}^k$ in most cases. For instance, the case of UPFC installation at the receiving end of line 5-6 is underlined in Tables 2 through 5; the difference between Δf_{sens}^k and $\Delta f_{\text{diffr}}^k$ is respectively 0.07, 2.68, 35.4 and 27.36 \$/hr. The effectiveness of the approximate results from the sensitivity analysis is further discussed in Section 4.4. Subsequently, the results of the differencing method for each step are reviewed.

4.1. Line Impedance Increase

From Table 2, it is evident that inserting the UPFC series transformer at either the sending end or the receiving end of a line produces roughly similar change in the OPF cost function. Furthermore, in most cases (13 cases out of 22), the OPF cost function increases when the UPFC series transformer impedance is inserted.

Table 2: OPF cost increase due to the addition of UPFC series part impedance.

line	impedance (pu)	sending end			receiving end		
		Δf_{difr}^1 (pu)	$\partial f/\partial X_s$ (\$/hr-pu)	Δf_{sens}^1 (pu)	Δf_{difr}^1 (pu)	$\partial f/\partial X_s$ (\$/hr-pu)	Δf_{sens}^1 (pu)
1-2	0.050	-8.52	-215.9	-10.79	-9.56	-251.7	-12.59
1-4	0.022	74.20	2549	56.60	80.07	2742	60.87
1-5	0.050	-4.73	-619	-30.96	-3.79	-697.8	-34.89
2-3	0.050	-1.52	-32.7	-1.64	1.12	30.46	1.52
2-4	0.022	-33.11	-3121	-69.28	-33.64	-3212	-71.31
2-5	0.089	59.54	472.9	42.04	72.89	540.2	48.03
2-6	0.010	3.92	354.6	3.51	4.59	411.1	4.07
3-5	0.016	4.25	217.8	3.55	5.07	259.5	4.23
3-6	0.013	4.78	295.7	3.70	4.83	295.9	3.70
4-5	0.200	-0.24	5.81	1.16	-14.60	-110.6	-22.12
5-6	0.050	3.23	67.27	3.36	0.69	12.41	0.62

4.2. Shunt Reactive Power Injection

By reviewing Δf_{difr}^2 in Table 3 and comparing the results of UPFC insertion on all lines connected to a particular bus, it may be concluded that connecting the UPFC to a certain bus, no matter on which line, would approximately lead to the same amount of shunt reactive compensation. For example, in installing the UPFC at the receiving end of line 2-3 and the sending ends of lines 3-5 and 3-6 in which the UPFC is connected to bus 3, Q_p takes very close values of 2.49, 3.85 and 3.63 \$/hr, respectively. Consequently, the results of Table 3 are grouped according to the buses not the lines. Also, it can be seen that whenever a UPFC is connected to one of the load buses, the OPF sets the shunt converter current, I_p , to its maximum value, that is 0.04 pu. These cases are marked by * in Table 3. This is due to the fact that by producing reactive power through a UPFC, active power loss as a result of reactive power flow on transmission lines would decrease.

4.3. Enabling U_{sx} and U_{sy}

The U_{sx} and U_{sy} compensation results are presented in Tables 4 and 5, respectively. The first and the second row of each line in both tables represent the results of placing UPFC at the sending and the receiving ends of the line, respectively. According to Tables 4 and 5, Δf_{difr}^3 and Δf_{difr}^4 are constantly negative; so, it may be concluded that enabling series voltage components would always cause the objective function of OPF to decrease. Also, it should be noted that the results of the sensitivity analysis, Δf_{sens}^3 and Δf_{sens}^4 , are usually greater than the differencing results, Δf_{difr}^3 and Δf_{difr}^4 ; the exception cases are shown in bold highlighting. Hence, it seems that by moving away from the initial operating point, the compensation slopes of the in-phase and the quadrature components decrease. An important thing to note is that U_{sx}^* at the sending end of a line is often very close to $-U_{sx}^*$ at its receiving end. For example, the U_{sx}^* values in Table 4 for the sending and the receiving ends of line 2-3 are

Table 3: Shunt reactive power compensation in 22 UPFC placement cases.

UPFC On bus	Line of UPFC	Q_p (MVAR)	Δf_{difr}^2 (\$/hr)	$\partial f / \partial Q_p$ (\$/hr·MVAR)	Δf_{sens}^2 (\$/hr)
1	1-2	0	0	0	0
	1-4		0		
	1-5		0		
2	1-2	0	0	0	0
	2-3		0		
	2-4		0		
	2-5		0		
	2-6		0		
3	2-3	2.49	-7.05	-2.40	-5.96
	3-5	3.85	-7.61*		-9.22
	3-6	3.63	-6.73*		-8.70
4	1-4	3.88	-54.79*	-10.47	-40.61
	2-4		-11.64*		
	4-5		-25.07*		
5	1-5	3.77	-8.36*	-5.95	-22.43
	2-5		-45.76*		
	3-5		-18.37*		
	4-5		-9.69*		
	5-6		-17.33*		
6	2-6	3.77	-11.35*	-3.33	-12.56
	3-6		-10.39*		
	5-6		-9.88*		

+0.056 and -0.055, respectively. This is also true about U_{sy}^* . Thus, moving a UPFC from one end of a line to the other end appears to have low effect on the U_{sx}^* or U_{sy}^* absolute value.

Figure 7 can be used to examine the proposed approach, explaining the relationship between U_{sx}^* and U_{sy}^* settings and LMPs in an electricity market. It shows both active and reactive LMPs of each system bus (inside a box beside the bus). These LMPs are derived from the OPF on the base case system without UPFC. The illustrated arrows at both ends of each line show the directions of the active and reactive power flows as a result of U_{sy}^* and U_{sx}^* activation, respectively. Also, the magnitudes of the settings U_{sx}^* and U_{sy}^* presented in Tables 4 and 5 are shown above each arrow.

The first part of the proposed approach is now applicable to all 22 cases except the four cases of UPFC insertion on line 1-5 and line 2-4, in which the current is set to the maximum value. It is shown that the approach truly predicts all the cases for the U_{sx}^* and U_{sy}^* settings. Lines 1-5 and 2-4, drawn by bold lines in Figure 7, are operating at their current thermal limit. Thus, the second part of the proposed approach should be evaluated in these cases. Active and reactive powers flow from bus 2 to bus 4 and the chosen U_{sx}^* and U_{sy}^* values at both ends of this line cause the line current to reduce, verifying the proposed approach. This is also the case in line 1-5 for U_{sy}^* ; however, U_{sx}^* values in line 1-5 do not follow the approach and are

Table 4: Compensation of the series voltage in-phase component.

Line	U_{sx}^* (pu)	Δf_{diff}^3 (\$/hr)	$\partial f / \partial U_{sx}$ (\$/hr.pu)	Δf_{sens}^3 (\$/hr)
1-2	-0.034	-14.18	893	-30.35
	0.030	-11.64	-837	-24.69
1-4	0.058	-132.1	-5180	-302.51
	-0.059	-84.32	4744	-281.30
1-5	0.024	-6.03	1407	33.78
	-0.027	-0.75	-1256	34.04
2-3	0.056	-18.64	-1032	-58.22
	-0.055	-14.90	1041	-57.02
2-4	0.001	0	4788	4.79
	0.003	-1.31	-4507	-12.62
2-5	0.022	-55.51	-1841	-41.23
	-0.013	-24.59	1682	-22.20
2-6	0.044	-20.32	-1224	-53.49
	-0.020	-7.96	1137	-22.40
3-5	0.030	-8.52	-990	-30.01
	0.002	0	828	1.74
3-6	0.011	-2.22	-200	-2.16
	-0.013	-1.04	105	-1.38
4-5	-0.019	-8.89	1490	-28.30
	0.022	-9.72	-1530	-33.34
5-6	-0.043	-7.98	952	-40.57
	0.047	-11.61	-992	-47.01

depicted by double line arrows in Figure 7. These violations are not surprising because the OPF problem shows a high degree of nonlinearity. Altogether, it seems that both parts of the approach efficiently predict the relationship between UPFC series voltage components and LMPs in an electricity market.

4.4. Determination of UPFC Installation Candidate Points Using Total Effects of Components

The impacts of the four elements on the OPF cost function in 22 cases are summarized in the stacked column chart shown in Figure 8. There are two columns for each of the 11 transmission lines in the figure. The left and the right columns are associated with UPFC installation at the sending and the receiving ends of the line, respectively. Each column consists of four stacked columns related to the four elements. The first stacked column represents the impact of the series transformer impedance insertion, represented by a vertical arrow. This element in some cases, such as UPFC insertion on both sides of line 2-4, has a positive effect and in some other cases, such as UPFC installation on both sides of line 1-4,

Table 5: Compensation of the series voltage quadrature component.

line	U_{sy}^* (pu)	Δf_{difr}^4 (\$/hr)	$\partial f / \partial U_{sy}$ (\$/hr·pu)	Δf_{sens}^4 (\$/hr)
1-2	-0.057	-19.92	1222	-70.14
	0.059	-21.63	-1257	-74.13
1-4	0.022	-1.255	-2296	-50.74
	-0.031	-2.91	2860	-87.22
1-5	-0.037	0	1049	-38.82
	0.015	-3.738	-1212	-18.19
2-3	0.027	-2.617	-488	-13.27
	-0.026	-2.269	476	-12.38
2-4	-0.014	-6.408	2960	-41.14
	0.000	0	-3244	0.65
2-5	0.026	-15.51	-871	-22.47
	-0.047	-23.28	1051	-49.09
2-6	0.008	-0.294	-358	-2.87
	-0.026	-2.189	463	-12.17
3-5	0.005	-0.053	-325	-1.62
	-0.019	-1.922	442	-8.49
3-6	0.036	-7.876	-359	-12.74
	-0.047	-11.61	432	-20.35
4-5	-0.025	-4.219	648	-15.87
	0.028	-5.1	-673	-18.49
5-6	-0.051	-6.942	655	-33.34
	0.054	-7.075	-641	-34.43

has a negative effect on the cost saving. Other elements, however, have always positive effects.

The total compensation of UPFCs can be identified by comparing the total column heights. It can be seen that after enabling the four components, the OPF cost is reduced in all the 22 cases. Another important thing can be inferred from the values for the lines in which one end is a generation bus and the other end is a load bus, including lines 1-4, 1-5, 2-4, 2-6, 3-5 and 3-6. In these cases, it is observed that UPFC installation at the load bus end of the line is more beneficial at the generation bus end. The reason is that the reactive compensation is much more at the load bus end while the other components produce almost the same results at either end.

Six cases out of 22 in which UPFCs have produced the most improvement are marked by * in Figure 8. These six cases are associated with UPFC installation on both ends of lines 1-2, 1-4 and 2-4. Since simultaneous insertion of a UPFC at both ends of a line is unrealistic, candidate points to install UPFCs in the six bus system appear to be the receiving ends of lines 1-2, 1-4 and 2-4.

Figure 9 shows the results of the total UPFC cost reductions by both approaches, normalized based on their respective maximum values. It can be seen that both approaches

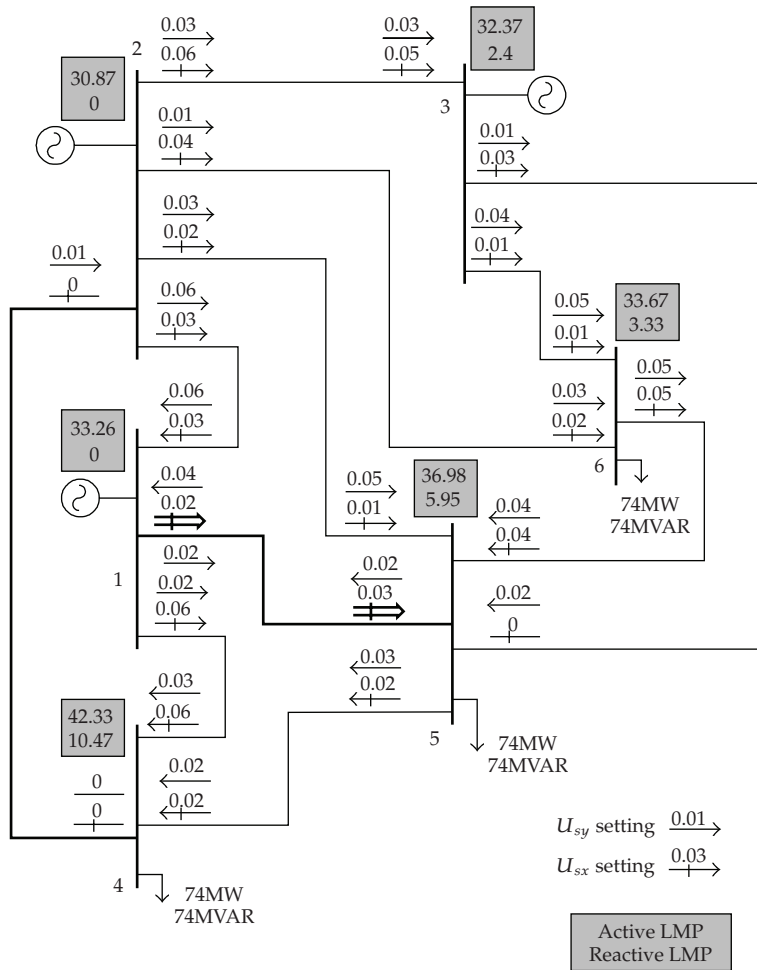


Figure 7: Active and reactive LMPs in the base case system and U_{sx}^* , U_{sy}^* settings for UPFC placement.

show the same pattern of compensation at different points of the system. Thus, it confirms the trustworthiness of the sensitivity approach. Furthermore, six points with the highest figures in the differencing and the sensitivity approaches are distinguished by * and + marks, respectively, in Figure 9. It is shown that the two approaches offer the same candidate points. Hence, the proposed sensitivity analysis seems to be, effectively, capable of determining the candidate points.

From a computational point of view, while the sensitivity method requires only one OPF run and some post studies, the differencing method needs much more calculations, that is, in our test case, 23 OPF runs, one for base case and 22 ones for UPFC installation on all lines. In order to assess how much saving can be obtained through UPFC installation, the cost of UPFC installation must be calculated. The cost of installation of UPFC is taken from Siemens database and reported in [18] given by (4.12).

$$C_{UPFC} = 0.0003S^2 - 0.2691S + 188.22, \tag{4.12}$$

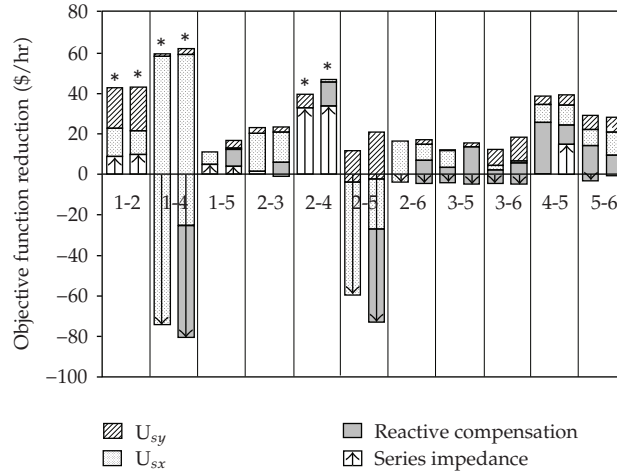


Figure 8: UPFC four elements compensation for 22 cases.

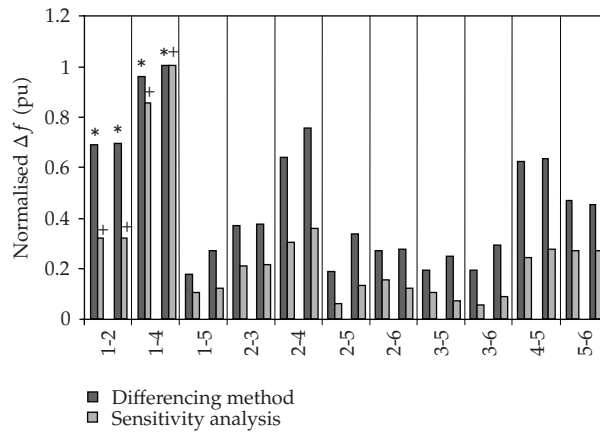


Figure 9: Results of UPFC total cost reduction by two approaches for 22 cases.

where C_{UPFC} is the cost of UPFC in US\$/kVA and S is the operating range of UPFC in MVA. Therefore, based on the supposed size of UPFC in our case studies, the cost of UPFC installation will be about 749,000\$. This cost will have to be compared with the revenue (or benefit) that can be derived from UPFC. The revenue derived from UPFC, shown in Figure 8, has the unit of “\$/hr” depending on the utilization and level of congestion. In order to compare the cost of FACTS against the anticipated benefits, they have to be converted to a common unit. In this paper, the comparison is made by converting the cost, as well as the benefit (or revenue) into annuity (“\$/year”). To compute the annual capital cost and benefit (revenue) of FACTS, following assumptions have been made:

Project lifetime (n): 5 years

Discount rate (r): 10%

Average utilization (u): 40%

Operational cost of FACTS device is neglected.

Annual capital cost of FACTS in \$/year can be found as [19]:

$$C_{UPFC}^{\text{Annual}} = C_{UPFC} \times S \times 1000 \times \frac{r \times (1+r)^n}{(1+r)^n - 1}. \quad (4.13)$$

Thus, the annual capital cost of UPFC in our test case is 197,000\$/year. Annual revenue from use of UPFC in \$/year can be determined as [19]:

$$R_{UPFC}^{\text{Annual}} = R_{UPFC}^{\text{hour}} \times 8760 \times u. \quad (4.14)$$

The average utilization u gives the percentage of time the UPFC device is considered 100% effective. Since, the demand and supply patterns change during different time period, leading to different price quantity relationship and consequently different setting for FACTS devices. At low load period, the effectiveness of UPFC devices decreases and hence the revenue (benefit) from use of UPFC decreases. So, to evaluate the benefit of UPFC a utilization factor is considered. Considering the best case, UPFC installation at the receiving end of line 1-4, the annual revenue generated due to UPFC is 217,000\$/year. Consequently, about US\$20,000 can be saved each year.

5. Conclusions

In this paper, a new explicit model for UPFC was proposed in which the parameters were assigned to the active and reactive power flows in the series and shunt parts of the UPFC. Using the proposed model, UPFC settings and power prices in a restructured power market were simultaneously determined to maximize the social welfare. Also based on the proposed model, impact of UPFC installation on the social welfare was considered to be the result of four elements.

By studying the test system with different UPFC positions, the effect of each element on the power market objective function was observed by means of a differencing method. Then, the total UPFC compensations in different cases were compared and suitable UPFC insertion points were suggested. The comparative results obtained by a sensitivity approach showed that two approaches offer almost the same candidate points in our case. Since the results of the sensitivity approach are calculated without repeating OPF solutions, the method is faster than the differencing method. Eventually, based on the functions of UPFC series voltage components, two rules for predicting the sign of these components in an electricity market were proposed and their effectiveness was practically confirmed by case studies.

Mathematical Symbols

Section 2: OPF Implementation

f (\$/hr)	An OPF cost function; an electricity market objective function
g	Equality constraints in OPF
h	Inequality constraints in OPF
t	A state variable in OPF
w	A control variable in OPF
P_{Gi} (MW)	The active power generation of generator- i

P_{Gi}^{\max} (MW)	The maximum active power generation of generator- i
P_{Gi}^{\min} (MW)	The minimum active power generation of generator- i
Q_{Gi} (MVAR)	The reactive power generation of generator- i
Q_{Gi}^{\max} (MVAR)	The maximum reactive power generation of generator- i
Q_{Gi}^{\min} (MVAR)	The minimum reactive power generation of generator- i
V_{Gi} (pu)	The voltage magnitude of generator- i
V_G^{\max} (pu)	The maximum allowable voltage for generators
V_G^{\min} (pu)	The minimum allowable voltage for generators
I_{i-j} (pu)	The magnitude of the current flowing through line $i-j$
I_{i-j}^{\max} (pu)	Maximum allowable current of line $i-j$
V_{Li} (pu)	The voltage magnitude of load bus- i
V_L^{\min} (pu)	The minimum allowable voltage for load buses
V_s^{\max} (pu)	The maximum allowable voltage for load buses
θ_{Li} (rad)	The voltage angle of load bus- i

Section 3: UPFC Modelling

\tilde{Z}_s (pu)	The leakage impedance of the series transformer
X_s (pu)	The leakage reactance of the series transformer
\tilde{Z}_p (pu)	The leakage impedance of the shunt transformer
I_s (pu)	The magnitude of The series converter current
I_p (pu)	The magnitude of The shunt converter current
Q_p (MVAR)	The net shunt reactive power injected to the former side bus
U_s (pu)	The amplitude of the series converter voltage
U_p (pu)	The amplitude of the shunt converter voltage
φ_s (rad)	The angle of the series converter voltage
φ_p (rad)	The angle of the shunt converter voltage
U_{sx} (pu)	The in-phase component of the series voltage
U_{sy} (pu)	The quadrature component of the series voltage
U_{px} (pu)	The in-phase component of the shunt voltage
U_{py} (pu)	The quadrature component of the shunt voltage
V_1 (pu)	The voltage magnitude of the former side bus
\tilde{V}_1 (pu)	The voltage phasor of the former side bus
V_2 (pu)	The voltage magnitude of the end side bus
δ_1 (rad)	The voltage angle of the former side bus
δ_2 (rad)	The voltage angle of the end side bus
I_s^{\max} (pu)	The maximum current of the series part
I_p^{\max} (pu)	The maximum current of the shunt part
U_s^{\max} (pu)	The maximum series voltage magnitude
U_p^{\max} (pu)	The maximum shunt voltage magnitude

Section 4: Case Studies and Results Analysis

MVA_{series} (MVA or pu)	The apparent power rating of the series converter in a UPFC
S_{base} (MVA)	The base value of system apparent powers
f_{opf}^k $k = 1, \dots, 4$ (\$/hr)	The OPF cost function determined in step k of the differencing method

Δf_{diff}^k $k = 1, \dots, 4$ (\$/hr)	The change in OPF cost function due to enabling an element y_k in the differencing method
f_{opf}^0 (\$/hr)	OPF cost function in a base case system with no UPFC
Δf_{sens}^k $k = 1, \dots, 4$ (\$/hr)	The estimated change in OPF cost function due to enabling an element y_k in the sensitivity method
y_k $k = 1, \dots, 4$	One of four UPFC elements effective in changing the OPF cost function
y_k^* $k = 1, \dots, 4$	The value of y_k determined in an OPF solution
$y_1^* = X_s$ (pu)	The series transformer leakage reactance of a UPFC
$y_2^* = Q_p$ (MVAR)	The net reactive power injected by the shunt converter of a UPFC obtained by OPF
$y_3^* = U_{sx}^*$ (pu)	The in-phase component of the series voltage in a UPFC obtained by OPF
$y_4^* = U_{sy}^*$ (pu)	The quadrature component of the series voltage in a UPFC obtained by OPF
$\partial f / \partial y_k$	The OPF cost function sensitivity with respect to an element y_k
V_i (pu)	The voltage magnitude at bus- i
$\Delta \delta$ (rad)	The difference between the voltage angles at buses 1 and 2
r_{12} (pu)	The resistance of line 1-2
x_{12} (pu)	The reactance of line 1-2
g_{12} (pu)	The conductance of $(r_{12} + jx_{12})$
b_{12} (pu)	The susceptance of $(r_{12} + jx_{12})$
B (pu)	The shunt susceptance of line 1-2
ALMP ₁ (\$/hr·MW)	The active LMP at bus-1
RLMP ₁ (\$/hr·MVAR)	The reactive LMP at bus-1
ALMP ₂ (\$/hr·MW)	The active LMP at bus-2
RLMP ₂ (\$/hr·MVAR)	The reactive LMP at bus-2
$\lambda_{I_{1-2}}$ (\$/hr·pu)	The Lagrangian multiplier of the maximum current constraint at the sending end of line1-2
$\lambda_{I_{2-1}}$ (\$/hr·pu)	The Lagrangian multiplier of the maximum current constraint at the receiving end of line1-2
I_t (pu)	The in-phase component of the shunt converter current with respect to \tilde{V}_1
I_q (pu)	The quadrature component of the shunt converter current with respect to \tilde{V}_1
S_{11-2} (MVA)	The apparent power through line 1-2 at its sending end when the UPFC is disabled
$P_{12\text{old}}$ (MW)	The active power flow at the sending end of line 1-2 when the UPFC is disabled
$Q_{12\text{old}}$ (MVAR)	The reactive power flow at the sending end of line 1-2 when the UPFC is disabled
$P_{21\text{old}}$ (MW)	The active power flow at the receiving end of line 1-2 when the UPFC is disabled
$Q_{21\text{old}}$ (MVAR)	The reactive power flow at the receiving end of line 1-2 when the UPFC is disabled

References

- [1] X.-P. Zhang and E. J. Handschin, "Advanced implementation of UPFC in a nonlinear interior-point OPF," *IEE Proceedings: Generation, Transmission and Distribution*, vol. 148, no. 5, pp. 489–496, 2001.
- [2] K. S. Verma, S. N. Singh, and H. O. Gupta, "Location of unified power flow controller for congestion management," *Electric Power Systems Research*, vol. 58, no. 2, pp. 89–96, 2001.
- [3] B. Venkatesh, M. K. George, and H. B. Gooi, "Fuzzy OPF incorporating UPFC," *IEE Proceedings: Generation, Transmission and Distribution*, vol. 151, no. 5, pp. 625–629, 2004.
- [4] S. Y. Ge and T. S. Chung, "Optimal active power flow incorporating power flow control needs in flexible AC transmission systems," *IEEE Transactions on Power Systems*, vol. 14, no. 2, pp. 738–744, 1999.
- [5] K. S. Verma and H. O. Gupta, "Impact on real and reactive power pricing in open power market using unified power flow controller," *IEEE Transactions on Power Systems*, vol. 21, no. 1, pp. 365–371, 2006.
- [6] M. I. Alomoush, "Impacts of UPFC on line flows and transmission usage," *Electric Power Systems Research*, vol. 71, no. 3, pp. 223–234, 2004.
- [7] A. J. Wood and B. F. Wollenberg, *Power Generation, Operation and Control*, John Wiley & Sons, New York, NY, USA, 2nd edition, 1996.
- [8] D. Kirschen and G. Strbac, *Fundamentals of Power System Economics*, John Wiley & Sons, New York, NY, USA, 1st edition, 2004.
- [9] L. Gyugyi and C. D. Schauder, in *Flexible AC Transmission Systems (FACTS)*, Y. H. Song and A. T. Johns, Eds., The Institution of Engineering and Technology (IET), pp. 268–311, IET, London, UK, 1999.
- [10] H. Ambriz-Pérez, E. Acha, C. R. Fuerte-Esquivel, and A. De la Torre, "Incorporation of a UPFC model in an optimal power flow using Newton's method," *IEE Proceedings: Generation, Transmission and Distribution*, vol. 145, no. 3, pp. 336–342, 1998.
- [11] R. Palma-Behnke, L. S. Vargas, J. R. Perez, J. D. Nunez, and R. A. Torres, "OPF With SVC and UPFC modeling for longitudinal systems," *IEEE Transactions on Power Systems*, vol. 19, no. 4, pp. 1742–1753, 2004.
- [12] W. L. Fang and H. W. Ngan, "Optimising location of unified power flow controllers using the method of augmented Lagrange multipliers," *IEE Proceedings: Generation, Transmission and Distribution*, vol. 146, no. 5, pp. 428–434, 1999.
- [13] M. Saravanan, S. M. R. Slochanal, P. Venkatesh, and J. P. S. Abraham, "Application of particle swarm optimization technique for optimal location of FACTS devices considering cost of installation and system loadability," *Electric Power Systems Research*, vol. 77, no. 3-4, pp. 276–283, 2007.
- [14] M. R. Hesamzadeh, A. A. Abrishemi, N. Hosseinzadeh, and P. Wolfs, "A novel modelling approach for exploring the effects of UPFC on restructured electricity market," in *Proceedings of the 8th International Power Engineering Conference (IPEC '07)*, pp. 437–442, 2007.
- [15] A. G. Bakirtzis, P. N. Biskas, C. E. Zoumas, and V. Petridis, "Optimal power flow by enhanced genetic algorithm," *IEEE Transactions on Power Systems*, vol. 17, no. 2, pp. 229–236, 2002.
- [16] C. R. Fuerte-Esquivel, E. Acha, and H. Ambriz-Perez, "A comprehensive Newton-Raphson UPFC model for the quadratic power flow solution of practical power networks," *IEEE Transactions on Power Systems*, vol. 15, no. 1, pp. 102–109, 2000.
- [17] M. Rahman, M. Ahmed, R. Gutman, R. J. O'Keefe, R. J. Nelson, and J. Bian, "UPFC application on the aep system: planning considerations," *IEEE Transactions on Power Systems*, vol. 12, no. 4, pp. 1695–1701, 1997.
- [18] M. Saravanan, S. M. R. Slochanal, P. Venkatesh, and J. P. S. Abraham, "Application of particle swarm optimization technique for optimal location of FACTS devices considering cost of installation and system loadability," *Electric Power Systems Research*, vol. 77, no. 3-4, pp. 276–283, 2007.
- [19] N. Mithulanathan and N. Acharya, "A proposal for investment recovery of FACTS devices in deregulated electricity markets," *Electric Power Systems Research*, vol. 77, no. 5-6, pp. 695–703, 2007.